Child's Nerv Syst (2002) 18:426–439
DOI 10.1007/s00381-002-0607-y

FOCUS SESSION

Neuroimaging of thalamic tumors in children

Cesare Colosimo
Giuseppe Maria di Lella
Tommaso Tartaglione
Riccardo Riccardi

Received: 8 March 2002
Published online: 30 July 2002
© Springer-Verlag 2002

C. Colosimo (✉)
Neuroradiology Section,
Institute of Advanced Biomedical Technology,
Department of Clinical Sciences and Bio-Imaging, University G. d'Annunzio,
Via Colle dell'Ara, Campus Universitario,
66100 Chieti Scalo, Italy
e-mail: colosimo@radiol.unich.it
Tel.: +39-0871-3556901
Fax: +39-0871-3556930

C. Colosimo · G.M. di Lella · T. Tartaglione
Institute of Radiology, Catholic University,
Rome, Italy

R. Riccardi
Pediatric Oncology Unit,
Institute of Pediatrics, Catholic University,
Rome, Italy

Abstract *Introduction:* Thalamic tumors are typical deep brain tumors; their incidence is not precisely known because of the different definition criteria. However, taking only lesions arising in the thalami into consideration (and excluding those secondarily involving the thalami from adjacent structures) approximately 40% of thalamic tumors affect patients under 18 years of age and thalamic neoplasms account for 2–5% of all intracranial tumors in children. *Materials and methods:* In the present paper we have focused attention on the neuroimaging features of thalamic tumors in a pediatric population; based upon personal experience, we suggest a rational neuroradiological approach to the diagnostic evaluation, describe CT and MRI findings of the most common tumors, and attempt to define basic patterns in order to provide the most reliable "pathological" diagnosis.

Keywords Thalamic tumors · Brain gliomas · Astrocytomas · Oligodendrogliomas · Computed tomography · Magnetic resonance imaging

Introduction

The thalami represent approximately 2% of the brain volume and 1–5% of brain tumors [6]. They are predominantly astrocytic neoplasms [4] and their deep location makes them difficult to treat, mainly because surgery is rarely feasible [3, 4, 6, 7, 13, 14, 22]; despite the introduction of modern computer/imaging-assisted procedures (neuronavigation/computer-assisted volumetric resection), [13] substantial tumor removal remains unfeasible in most instances, while radiation therapy – with or without adjuvant chemotherapy [1, 18] – is still considered to be the basic treatment. Thalamic neoplasms are slightly more common in children [1, 25] than in adults and involve significant diagnostic, prognostic, and therapeutic problems. Modern neuroimaging techniques have substantially improved the possibilities of correct noninvasive characterization and staging of these deep-seated lesions, and they have provided optimal assistance for guiding stereotactic biopsy [13], neuronavigation and surgical attempts [5, 19, 22], and allowing a reliable evaluation of the effects of the applied therapy. This paper attempts to give an update on the neuroimaging techniques that are feasible in children affected by thalamic tumors by focusing on the following three steps: tailoring the general technical approach and semeiotics that are to be applied to thalamic neoplasms in children; describing the imaging features of the most common oncotypes in pediatric thalamic location; identifying basic neuroimaging patterns in order to guide the differential diagnosis.

Tailoring neuroimaging to thalamic tumors in children

Magnetic resonance imaging (MRI) has become the standard diagnostic tool for intracranial tumors. It is based on the application of different imaging sequences (essentially T1- and T2-weighted images), and on intravenous contrast medium administration. Computed tomography (CT) is still preferred in emergencies and for distinctly detecting intratumoral calcifications, while iodine-enhanced studies should no longer be considered useful [24, 25]. When faced with a suspected thalamic tumor, Flow-Attenuated Inversion Recovery (FLAIR) and heavily T1-weighted Inversion Recovery (IR) sequences should be added to conventional Spin Echo (SE) and Turbo-Spin Echo (TSE) sequences; thin slice (3 mm) FLAIR and IR images can be acquired with short acquisition times using the TSE option, improving the definition of lesion margins with adjacent CSF spaces (FLAIR) and critical deep structures such as internal capsule, midbrain nuclei and tracts, and other basal ganglia (IR). Moreover, the frequent need for biopsy and neuronavigation [13] makes volumetric studies mandatory; they are usually obtained using magnetization-prepared gradient-echo sequences (variously named as MP-RAGE, SPGR) that allow good resolution ≈1 mm-thick, over-contiguous, heavily T1-weighted (T1-WI), and produce optimal 2D multiplanar and 3D reconstructions. The sensitivity to contrast enhancement detection may be increased by using the magnetization transfer contrast (MTC) technique, which lowers the background signal, especially in the white matter. As far as a tailored evaluation is concerned, the new non-anatomical ("functional") MRI-based techniques should be kept in mind: perfusion-weighted imaging (PWI) and spectroscopy may usefully be included in selected instances. Basically, PWI looks at the evaluation of the regional blood volume; it is obtained after paramagnetic contrast medium bolus injection as a first-pass study, generating a concentration/time curve and several parameters (first arrival, mean transit and time to peak times, blood volume and flow). PWI is aimed at trying an additional way of assessing tumor anaplasia, assuming that the blood volume (and capillary bed) is increased in malignant lesions. Clinical experience is still limited: many reports advocate a good correspondence between blood volume and malignancy, but many limitations and exceptions are also reported (i.e., benign lesions have high blood volume and malignant lesions exhibit a relatively low blood volume). MR spectroscopy (MRS) has recently entered daily clinical practice, thanks to the introduction and diffusion of commercially available coils and software packages. The technique tends toward tissue characterization by displaying graphs that represent the level of the main neuro-metabolites; recently it has been possible for this level to be displayed as shades of gray producing the spectroscopic images. Clinical spectroscopy uses two main techniques: PRESS (point-resolved surface coil spectroscopy) and STEAM (stimulated echo method). The signal from water protons is usually reduced using suitable techniques, and results may be displayed in one, two or three dimensions; two-dimensional spectroscopy is more commonly used due to the extremely long acquisition times required for three-dimensional studies. MRS application in neoplastic diseases is intended to define the degree of malignancy on the basis of certain metabolites: the most significant data concerns choline, creatine, lactate and N-acetyl-aspartate. The choline level is of paramount importance because its elevation indicates a high degree of membrane metabolism that usually takes place in highly proliferating malignant tumors [9, 12]. On the other hand, a lactate increase is observed in necrotic lesions; this was found in both necrotic glioblastoma multiformis and in non-neoplastic lesions characterized by necrosis. The MR-based tumor characterization mentioned above appears to be extremely useful in deep-seated lesions in which tissue sampling requires sophisticated, invasive, and potentially hazardous surgical approaches; therefore both PWI and MRS have recently been used in children with thalamic gliomas [9]. Moreover, PWI and MRS were also used to evaluate the response of thalamic tumors to radiation and to differentiate between radiation-induced necrosis and tumor recurrence [17, 20].

Other recently introduced non-structural/functional MR-based techniques appear to be only marginally useful in thalamic tumors. Diffusion-weighted imaging (DWI) can help in the differential diagnosis between necrotic tumors and deep abscesses. Functional MRI (f-MRI) is difficult to apply in children, and even in adolescents it is limited because of the lack of a specific activation task.

A complete neuroradiological evaluation of brain tumors should achieve the following main results: the distinct detection of a neoplastic lesion, the precise definition of its extent, and the formulation of a reliable histological diagnosis. Such ideal results can be accomplished by a rational step-by-step analysis of CT/MRI findings: the detection of abnormal tissue (CT density, MR signal, abnormal contrast enhancement), the definition of the lesion site and extent, the recognition of mass effects, the exclusion of non-neoplastic diseases, the characterization of the lesion, and the proposal of a possible histological diagnosis. The latter is usually the result of matching characterization with clinical findings.

As in other brain tumors, the detection of thalamic neoplasms is more accurate on T2-weighted images (T2-WI), using both SE/TSE long TR/long TE and FLAIR images; the sensitivity of the images mentioned above is far superior to that of any T1-WI or CT scan. Using the multiplanar MRI evaluation, the epicenter of the lesion can be distinctly located within the thalamus; the extent

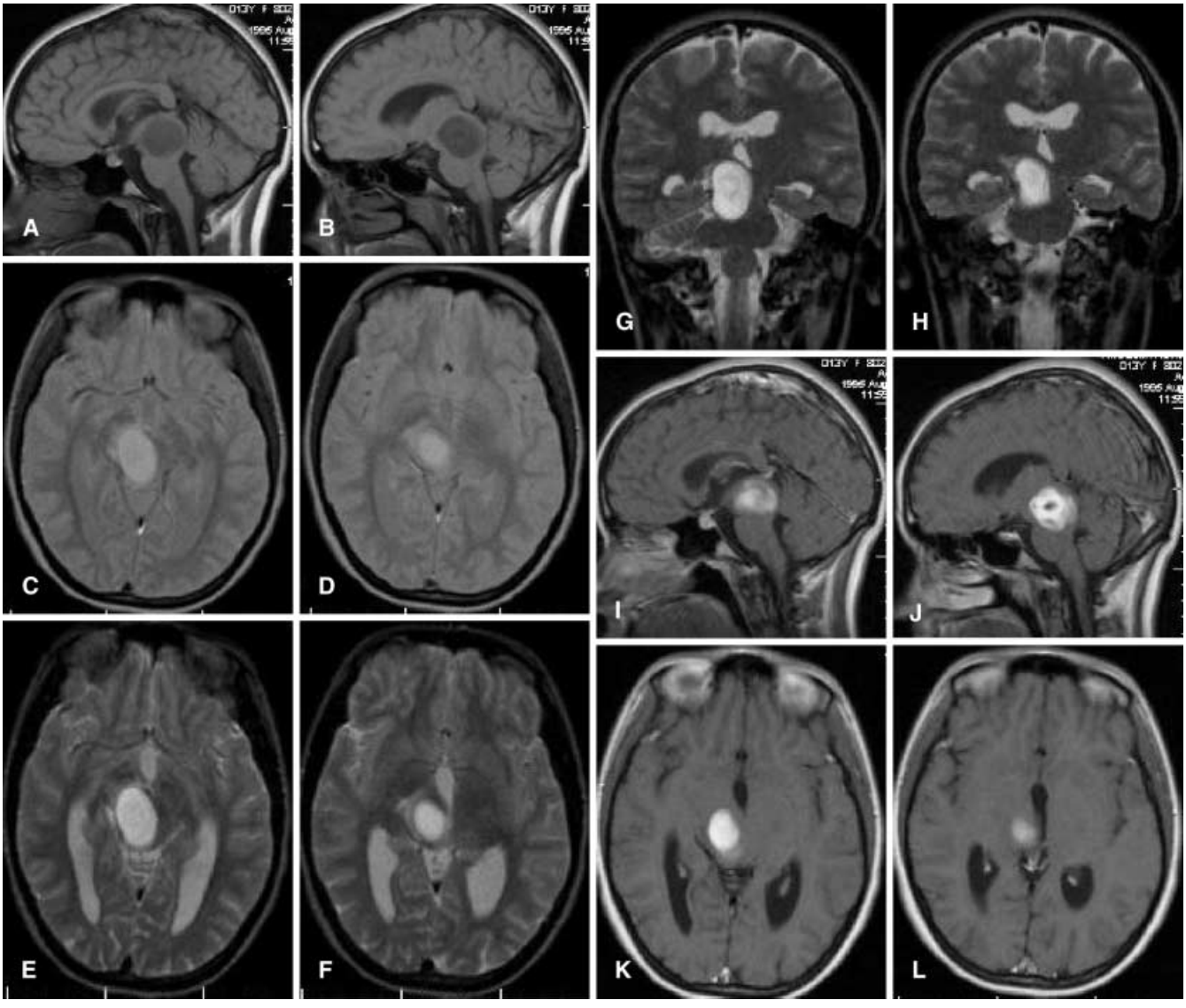

Fig. 1A–L Thirteen-year-old female; right thalamic pilocytic astrocytoma. **A**, **B** Sagittal SE T1-WI. **C–F** Axial SE PD- and T2-WI. **G**, **H** Coronal FSE T2-WI. **I–L** Sagittal and axial SE T1-WI after contrast injection. The tumor shows well-defined margins and appears hypointense on T1-WI, hyperintense on T2-WI, with minimal edema and intense contrast enhancement; the posterior portion of the third ventricle is displaced contralaterally

of the disease in the thalamus involved and in the adjacent structures can be assessed.

A mass effect due to the neoplastic enlargement of the thalamus and related edema usually results in the displacement and/or effacement of adjacent CSF spaces (third ventricle, ventricular atrium, lateral ventricular body, ambiens cisterns), and displacement of the internal capsule and basal ganglia.

Less frequently, hydrocephalus results from distortion of the posterior third ventricle and aqueduct; a mass effect on the ventricular trigone may induce incarceration of the temporal/occipital horns.

Unfortunately the exclusion of non-neoplastic diseases is not always possible: vascular diseases (both arterial ischemic and venous obstructive diseases), infectious/inflammatory diseases, metabolic (i.e., mitochondrial) processes, and even malformations may closely mimic thalamic tumors, thus requiring a careful analysis of CT/MRI findings.

The characterization of a thalamic tumor should follow the classic course, drawing macroscopic and even microscopic information from CT/MRI features of the lesion. The tumor should be separated from the adjacent edema (if present) and signal/density of the neoplastic tissue should be examined in order to detect solid and/or cystic areas, hemorrhage and their sequelae, and calcification. As in other locations, the solid tumor tissue should be carefully examined on T2-WI, focusing on its signal intensity, homogeneity, and above all on its mar-

Fig. 2A–C Twenty-four-month-old male; bilateral thalamic and basal ganglia pilocytic astrocytoma. **A** Axial SE T2-WI. **B**, **C** Axial and coronal SE T1-WI after contrast injection. Two large well-defined, lobulated thalamic and basal ganglia masses appear strongly hyperintense on T2-WI, with marked and inhomogeneous enhancement

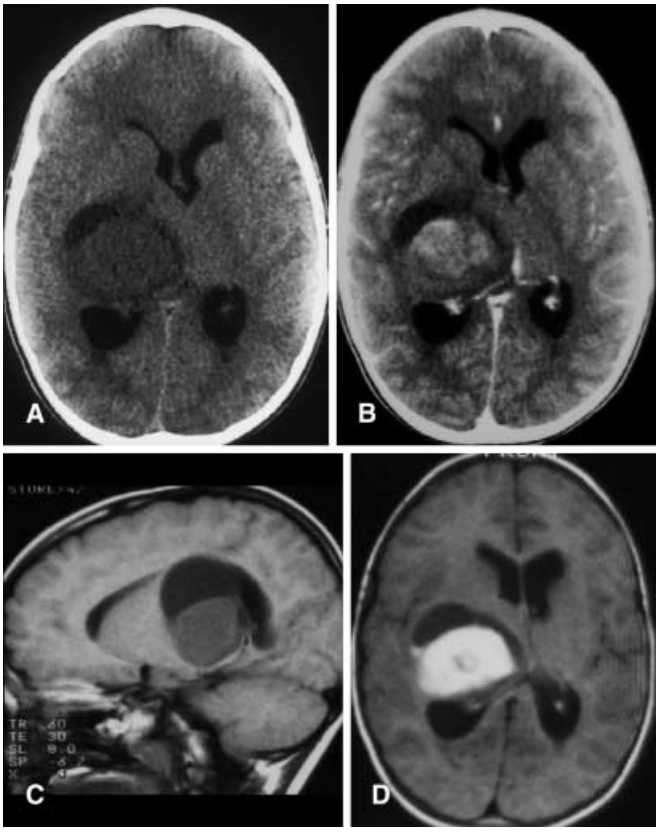

Fig. 3A–D Four-year-old male; right thalamic, partly cystic, pilocytic astrocytoma. **A**, **B** Axial CT before and after contrast injection. **C** Sagittal SE T1-WI. **D** Axial SE T1-WI after contrast injection. The well-defined mass, with peripheral cystic component is located in the right thalamus. The lesion is hypodense on pre-contrast CT scan with inhomogeneous enhancement after iodine injection. Note that degree of contrast enhancement is more pronounced on post-contrast MRI than on post-contrast CT; the cranial cystic component is better shown on sagittal images

gins. T2-WI high intensity indicates that the thalamic tumor has a microcystic constitution and/or low cellularity (see Figs. 1, 2, 4). These characteristics are usually found in most astrocytomas, while a relatively low intensity corresponds to high cellularity (see Figs. 9, 13, 15) or hemosiderin deposit (see Fig. 10). High cellularity thalamic tumors include germ cell tumors (see Fig. 15), lymphomas, and highly proliferating areas in malignant astrocytic (Figs. 9, 10) and embryonal tumors (Fig. 13). Similarly, non-homogeneity in a solid thalamic astrocytoma suggests possible anaplasia (Fig. 9) and the differentiation between true cysts and necrosis deserves the maximum attention because cysts are usually found in thalamic pilocytic astrocytomas (see Fig. 3) and oligodendrogliomas, whereas necrosis is almost specific of glioblastoma multiformis (Fig. 10).

The careful scrutiny of the margins (and extent) of the tumor is of paramount importance for thalamic tumors: lesions with sharp margins (circumscribed tumors) must be separated from those with ill-defined margins (infiltrating tumors). The infiltrating nature of a thalamic tumor is confirmed when there is a discrepancy between the volume and the mass effect of the lesion (relatively large tumors with relatively scarse mass effect). Ill-defined margins generally mean infiltration from the thalamic tumor that may involve the cerebral peduncles and the subthalamic structures, the posterior limbs of the internal capsule, and the ventricular ependyma (especially in germ cell tumors, lymphomas, and in some instances also in malignant astrocytomas).

Since multifocal/multicentric tumors are commonly encountered, contralateral thalamic and other basal ganglia lesions [25] should be excluded and CSF seeding should be ruled out (on contrast-enhanced images) in cases with infiltration of the third ventricle (i.e., in germ cell/primitive neuroectodermal tumors and lymphomas) (Fig. 15).

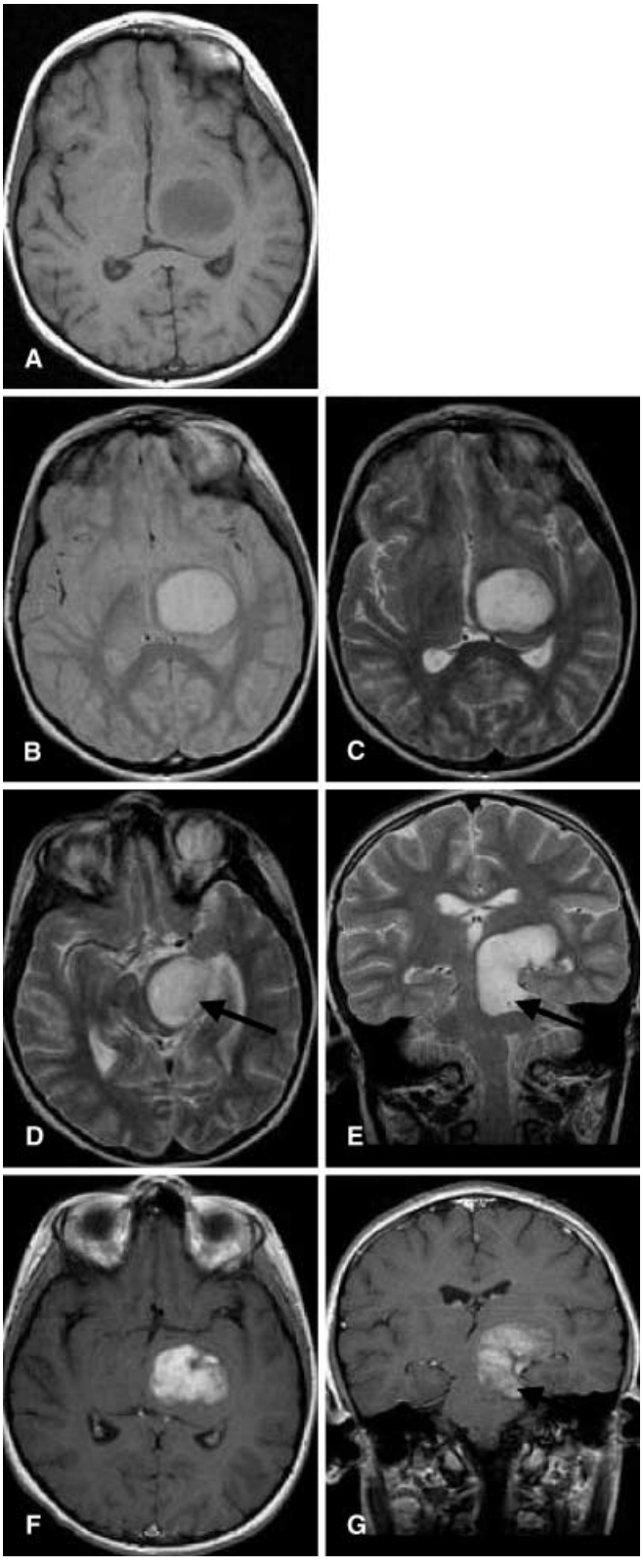

Fig. 4A–G Seven-year-old female; left thalamic pilocytic astrocytoma. **A** Axial SE T1-WI. **B, C–D** Axial SE PD- and T2-WI. **E** Coronal FSE T2-WI. **F**, **G** Axial and coronal SE T1-WI after contrast injection. The well-defined mass originates in the left thalamus and extends into the ipsilateral cerebral peduncle (*arrows* in **D**, **E**, **G**). The lesion is quite homogeneous on pre-contrast images, with slightly hypointensity on T1-WI, hyperintensity on PD and T2-WI; after contrast injection the lesion shows inhomogeneous enhancement

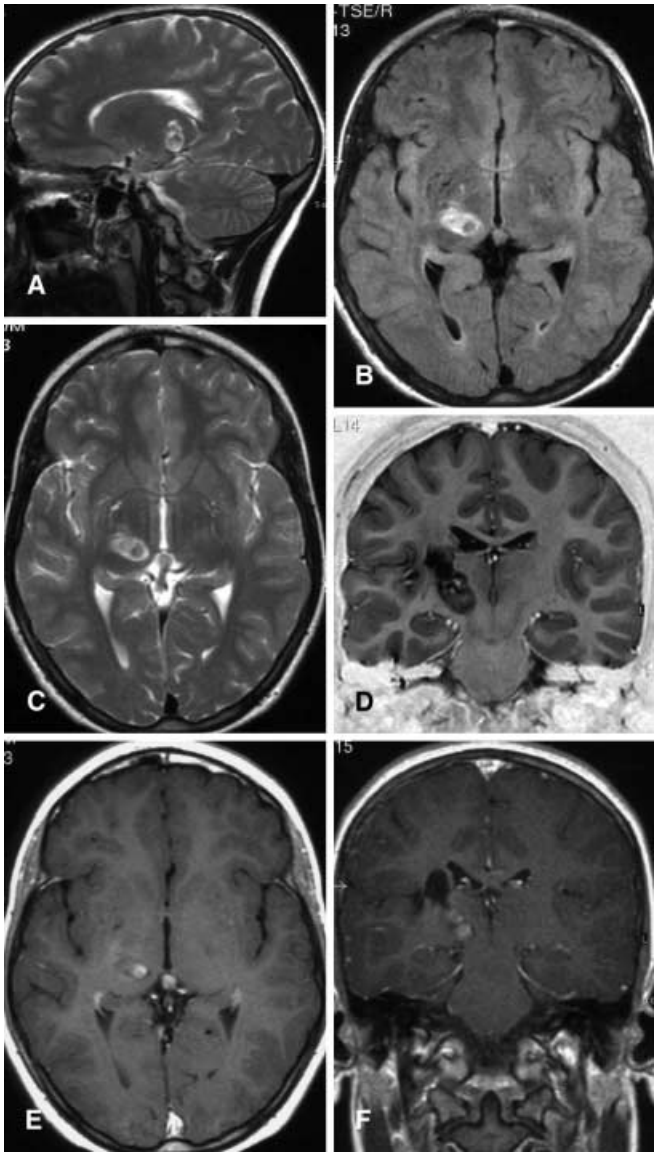

Fig. 5A–F Twelve-year-old female; residual pilocytic astrocytoma after partial resection. **A** Sagittal FSE T2-WI. **B** Axial FLAIR T2-WI. **C** Axial SE T2-WI. **D** Coronal IR T1-WI. **E**, **F** Axial and coronal SE T1-WI after contrast injection. The MR scan, obtained 1 year after partial resection of the tumor shows the well-defined residual tumor that appears located deep in the CSF-filled surgical cavity. The small mass also appears quite inhomogeneous in the pre-contrast T2-WI, and shows poor enhancement in post-contrast MR images

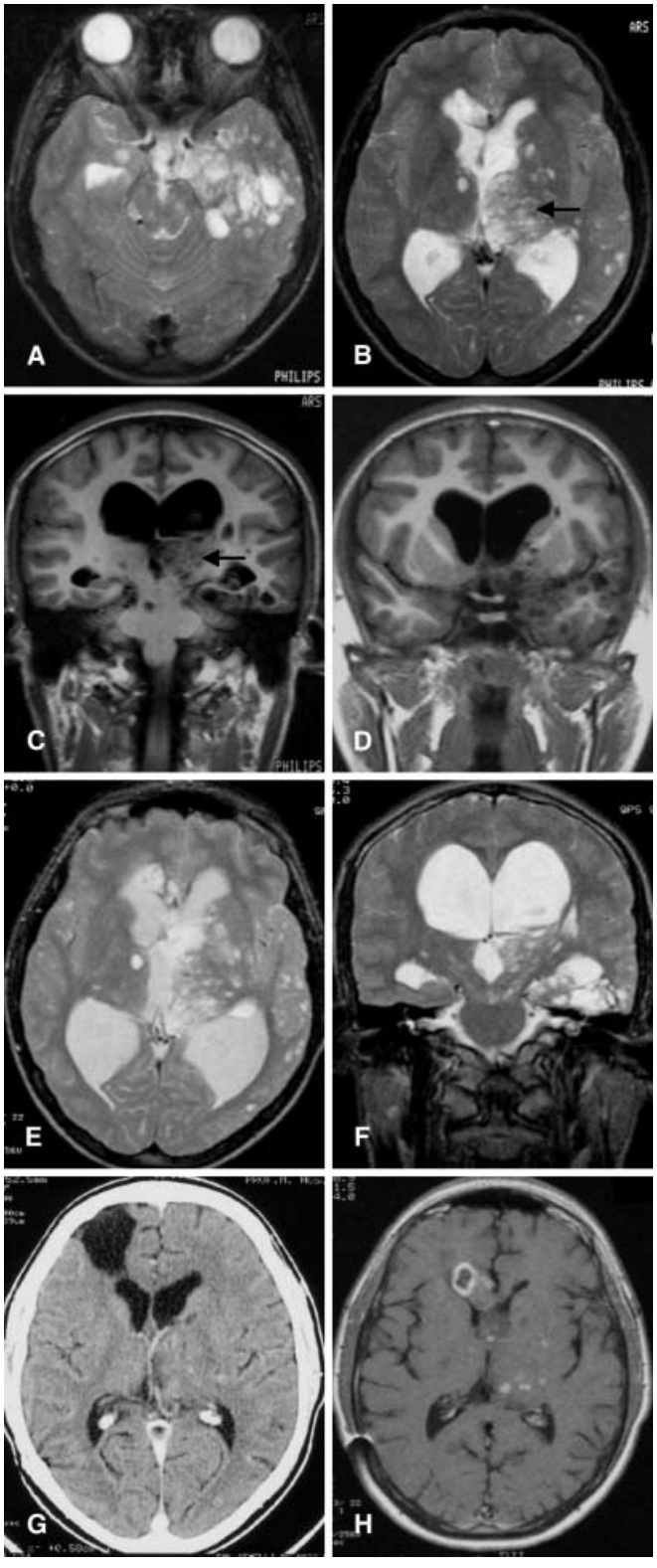

Fig. 6A–H Fourteen-year-old male; multifocal diffuse low-grade astrocytoma involving the left thalamus. **A**, **B** Axial SE T2-WI. **C**, **D** Coronal IR T1-WI. **E**, **F** One-year control: axial and coronal SE and FSE T2-WI. **G** Two-year control: axial CT scan after contrast injection. **H** Three-year control: axial SE T1-WI after contrast injection. Multiple rounded lesions hypointense on T1-WI, with bright signal on T2-WI, are located in both hemispheres, particularly in the left temporal lobe. An ill-defined mass (*arrow*) involves the left thalamus and the adjacent posterior limb of internal capsule. Mass effect on the posterior third ventricle and aqueduct results in hydrocephalus. The 1-year follow-up study (after surgical biopsy) does not show significant modifications of both the thalamic and hemispheric lesions. Further follow-up examinations do not show any significant growth of the lesions; some of the locations demonstrate nodular or peripheral enhancement

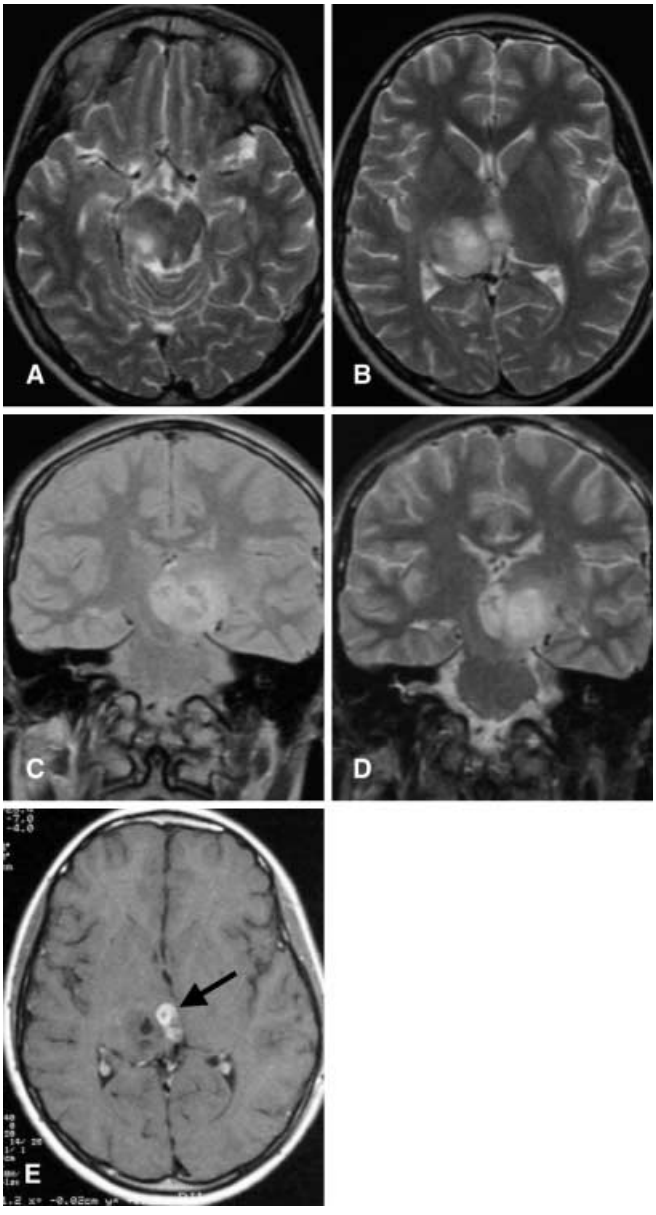

Fig. 7A–E Ten-year-old female; anaplastic astrocytoma of the right thalamus. **A**, **B** Axial SE T2-WI. **C**, **D** Coronal SE PD- and T2-WI. **E** Axial SE T1-WI after contrast injection. The right thalamic tumor is heterogeneous on both long TR and on post-contrast images; the margins are poorly defined and contrast enhancement of the medial component is inhomogeneous (*arrow*)

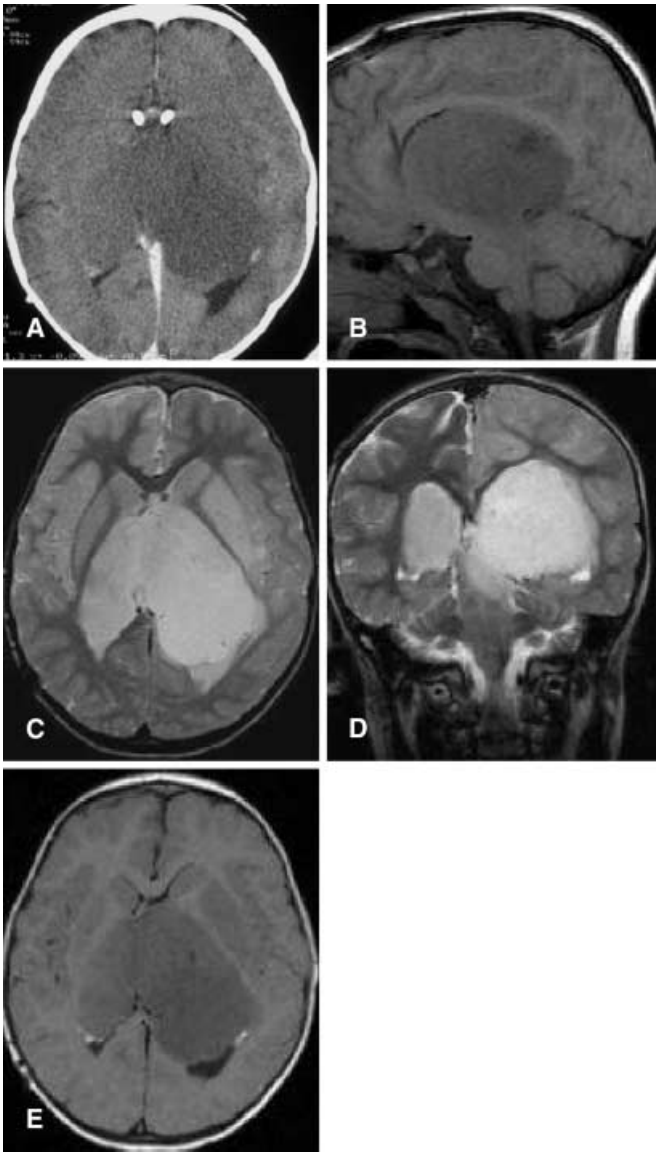

Fig. 8A–E Seven-year-old male; bilateral thalamic anaplastic astrocytoma. **A** Axial CT scan after contrast injection. **B** Sagittal SE T1-WI. **C**, **D** Axial and coronal SE T2-WI. **E** Axial SE T1-WI after contrast injection. Both thalami are swollen, particularly the left one. The neoplastic tissue is hypodense on CT, hyperintense on T2-WI, without enhancement on post-contrast T1-WI. The tumors appear rather homogeneous and well marginated. The third ventricle is compressed and displaced to the right. Double shunts have been inserted to treat hydrocephalus

Imaging features of the most common thalamic tumors

Thalamic tumors are generally considered together with basal ganglionic tumors, although the thalami are part of the diencephalon. Comprehensively, basal ganglia and thalamic tumors account for 10% of supratentorial tumors in children and nearly two-thirds of these neoplasms involve the thalami. Most thalamic tumors are astrocytomas [23], which are characterized not only by GFAP positivity, but also by extreme differences in morphology (histology), biological and clinical behavior, prognosis, and imaging findings. Thalamic locations are common in multifocal/multicentric astrocytic tumors and in gliomatosis cerebri [10]. In thalami, oligodendrogliomas, mixed gliomas, neuronal and mixed astrocytic/neuronal, and atypical teratoid-rhabdoid tumors are much less frequently found. Non-neuroepithelial tumors can be localized in the thalami: primitive lymphomas and germ cell tumors are the most common. The latter usually arise in the anterior or posterior (pineal) third ventricle, but frequently involve the medial thalamic nuclei directly and form true thalamic masses.

Pilocytic astrocytomas

In the thalami, pilocytic astrocytomas (PA) are much less frequent than in the cerebellum, optic-chiasmatic region, and cerebral hemispheres. PA represent the prototype of benign circumscribed astrocytomas, usually without a tendency to infiltrate and progress toward anaplasia. CT/MRI features are characterized by the well-circumscribed appearance, with sharp margins, and variable size, mass effect, and degree of the perilesional edema. The tumor is predominantly solid, largely cystic, or mixed. The typical cerebellar presentation as a cystic tumor with a mural nodule or a thick solid rim is rarely encountered in the thalami, where solid tumors predominate, with or without small cystic areas. The solid portion of PA is usually moderately hyperintense on T2-WI, faintly hypointense or isointense on TI-WI, with bright enhancement after contrast injection (Figs. 1, 2, 3, 4, 5). Calcification is not uncommon and sometimes intratumoral hemorrhages are found. In summary, the inhomogeneity of PA may lead to the suspicion of malignant astrocytoma, but the well-defined margins, the bright contrast enhancement, and the lack of necrosis usually lead to a correct pre-operative diagnosis.

Diffuse astrocytomas and anaplastic astrocytomas

Non-anaplastic astrocytomas are more commonly fibrillary astrocytomas (Figs. 6, 7) and less frequently protoplasmatic astrocytomas; despite the lack of anaplastic features they have the intrinsic tendency to infiltrate the adjacent tissue and progress toward anaplasia. Astrocytomas are usually heterogeneous tumors and in the same lesion various degrees of cellularity, mitoses, and vascularity are observed. Thus a precise differentiation between diffuse astrocytomas (A) and anaplastic astrocytomas (AA) is not feasible and the neuroradiological features are considered separately.

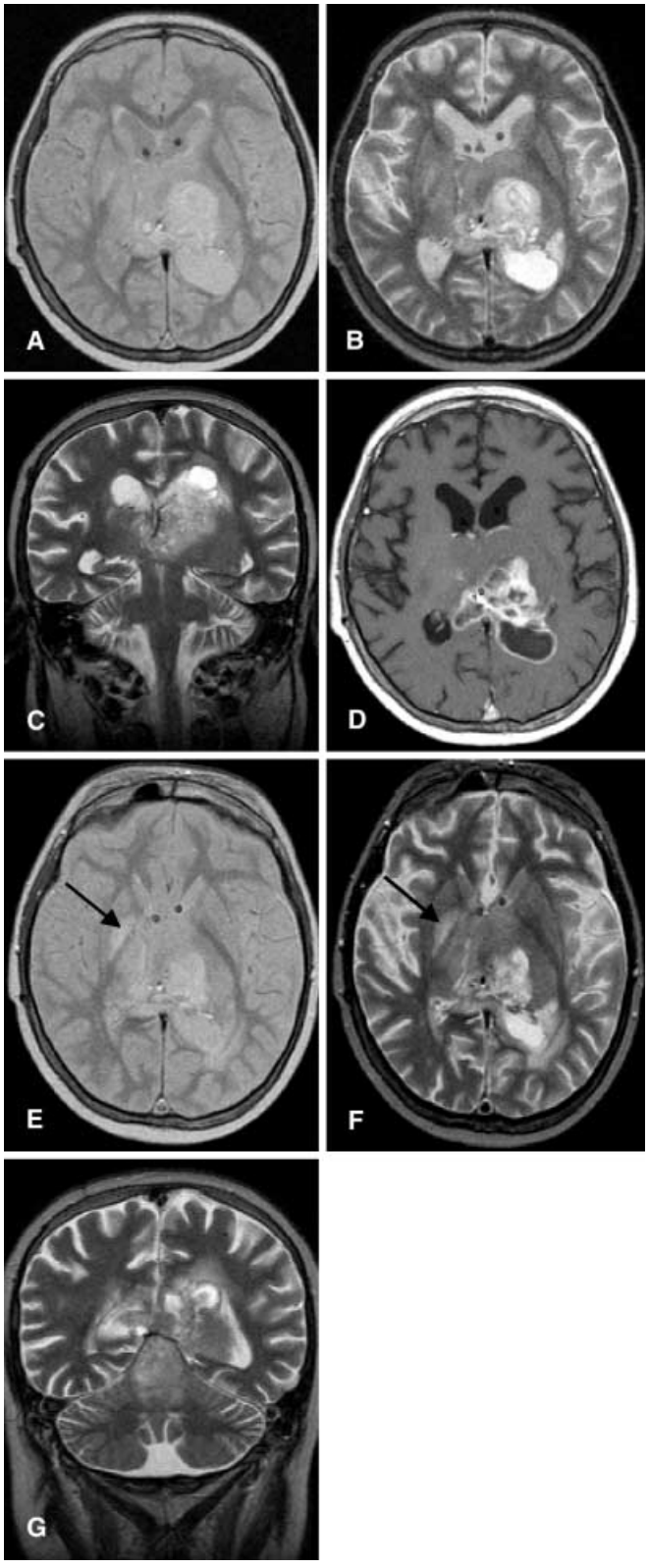

Fig. 9A–G Thirteen-year-old male; anaplastic astrocytoma of the left thalamus. **A**, **B** Axial SE PD and T2-WI. **C** Coronal FSE T2-WI. **D** Axial SE T1-WI after contrast injection. **E**, **F** Follow-up axial SE PD- and T2-WI. **G** Follow-up coronal FSE T2-WI. The poorly marginated, highly heterogeneous lesion, originating from the left thalamus extends (possibly via the adhesio interthalamica) into the medial nuclei of the contralateral thalamus and infiltrates the adjacent ventricular structures and corpus callosum. Bilateral shunts are inserted. The 5-month follow-up study demonstrates enlargement of the right thalamic tumor, caudal growth in the infratentorial compartment, and a definite hyperintensity on long TR images in the right globus pallidus (*arrow* **E**, **F**)

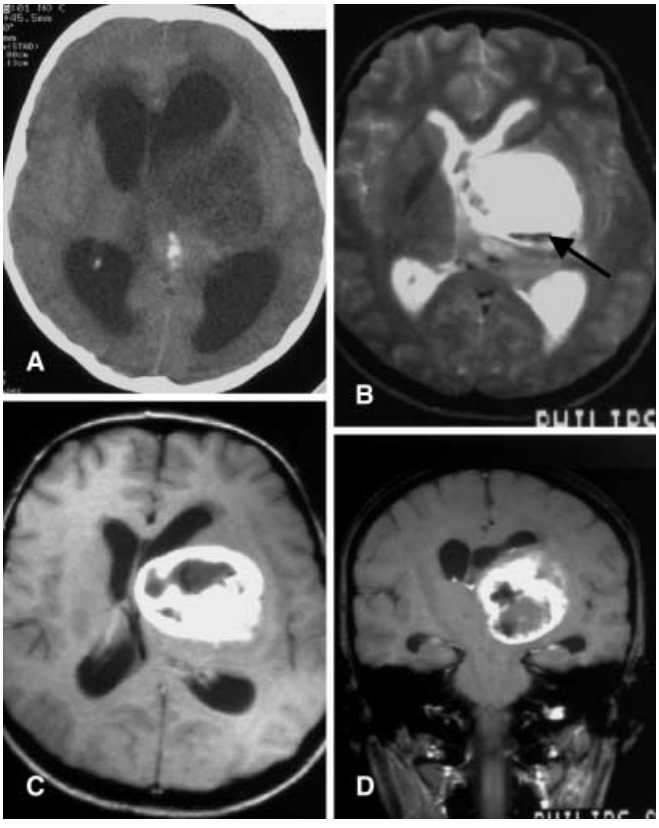

Fig. 10A–D Sixteen-year-old female; glioblastoma multiformis of left thalamus. **A** Unenhanced CT scan. **B** Axial SE T2-WI. **C**, **D** Axial and coronal SE T1-WI after contrast injection. A huge neoplastic lesion involving the left thalamus and basal ganglia region is clearly depicted on CT and MR images. The tumor is inhomogeneously hypodense on CT, hyperintense on T2-WI and with marked enhancement after gadolinium injection, because of central necrosis and hemorrhage (a fluid-fluid level is clearly evident, *arrow* in **B**). The patient survived acute lymphocytic leukemia and has been treated with combined chemotherapy and radiation on the cranio-spinal axis as meningeal prophylaxis; thus the lesion may be considered to be radiation-induced

In the author's experience A and AA represent the most common thalamic tumors in children. The low-grade (or non-anaplastic) A (Fig. 8) show diffuse increased signal on T2-WI, while signal modification (hypointensity) on T1-WI is constantly less prominent, and there is no contrast enhancement. The lesion results in the enlargement of the entire thalamus involved, while appar-

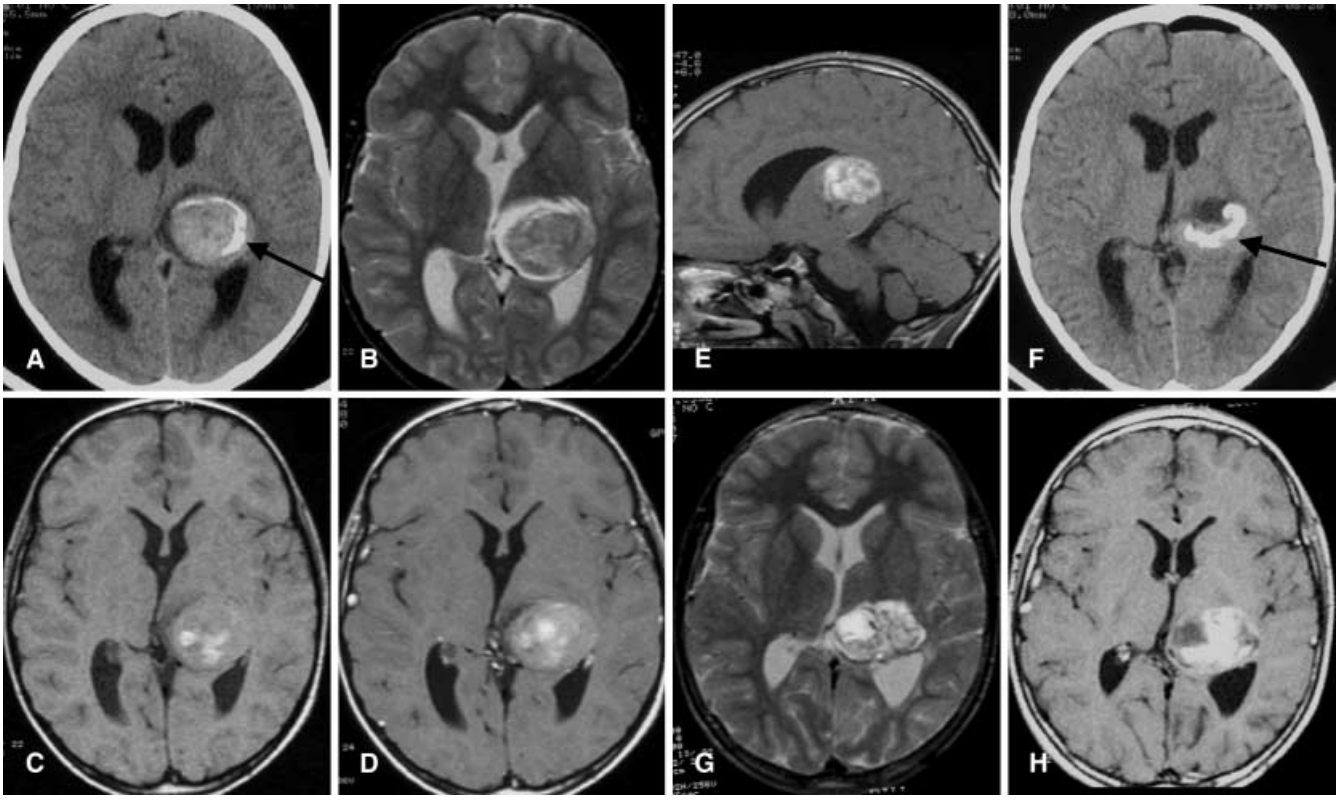

Fig. 11A–H Seven-year-old female; oligodendroglioma of the left thalamus. **A** Axial CT scan. **B** Axial SE T2-WI. **C** Axial SE T1-WI. **D**, **E** Axial and sagittal SE T1-WI after contrast injection. **F** Post-operative axial CT scan after contrast injection. **G** Post-operative axial SE T2-WI. **H** Post-operative axial SE T1-WI after contrast injection. A rounded well-circumscribed mass, with peripheral calcification (*arrow* in **A**, **F**), is located in the upper portion of the left thalamus. The lesion appears slightly isodense on CT, inhomogeneously hypointense on T2-WI, with little central hemorrhagic foci (hyperintense on T1-WI), and mild enhancement after contrast injection. The post-operative examinations demonstrate the partial resection of the tumor, while the CT scan shows the residual peripheral calcifications

ently sparing the adjacent white matter. A more detailed study of TSE, FLAIR and IR images usually reveals marginal infiltration as ill-defined signal changes that shade in the subthalamic areas, the cerebral peduncles or the internal capsule. Perilesional edema is usually lacking or extremely limited, thus nearly all the signal alterations seen on T2-WI correspond to neoplastic tissue.

On the other hand the typical features of AA are the inhomogeneity of the thalamic signal modification (both on T2- and T1-WI) due to variable cellularity and vascularity, the presence of non-homogeneous contrast enhancement, and extensive edema (Fig. 9). Obviously, in such cases a precise differentiation between tumor infiltration and edema may not be feasible, although the signal of infiltrated tissue tends to be lower than that of reactive edema. Thus inhomogeneity, irregular contrast enhancement, and extensive edema should be considered to be characteristic of anaplasia, but also the extensive infiltrative growth is to be maintained as an indicator of malignancy and of dismal prognosis. When an abnormal tumor signal involves both thalami or extends from the thalamus to infiltrate the brainstem, the striatum, the capsules, or even the paraventricular white matter, the lesion should be regarded as malignant even when completely homogeneous and lacking contrast enhancement. In particular, bilateral thalamic astrocytomas represent an uncommon but easily recognized condition that implies a poor prognosis [25], as confirmed in another paper in the current volume of this journal.

Glioblastoma multiformis

Glioblastoma multiformis (GBM) is less common by far in children than in adults and in elderly patients; moreover, progression from astrocytoma to GBM is frequent in adults but exceptional in children. In the authors' experience pediatric GBM is more commonly encountered in children who have survived previous malignant neoplasms and had been treated with brain irradiation and/or chemotherapy [8]. Neurofibromatosis I carries a major risk of developing GBMs or other malignant gliomas in the first two decades of life. As is the case in the more common subcortical location in adults, thalamic GBM in children appears as a fairly localized mass lesion with

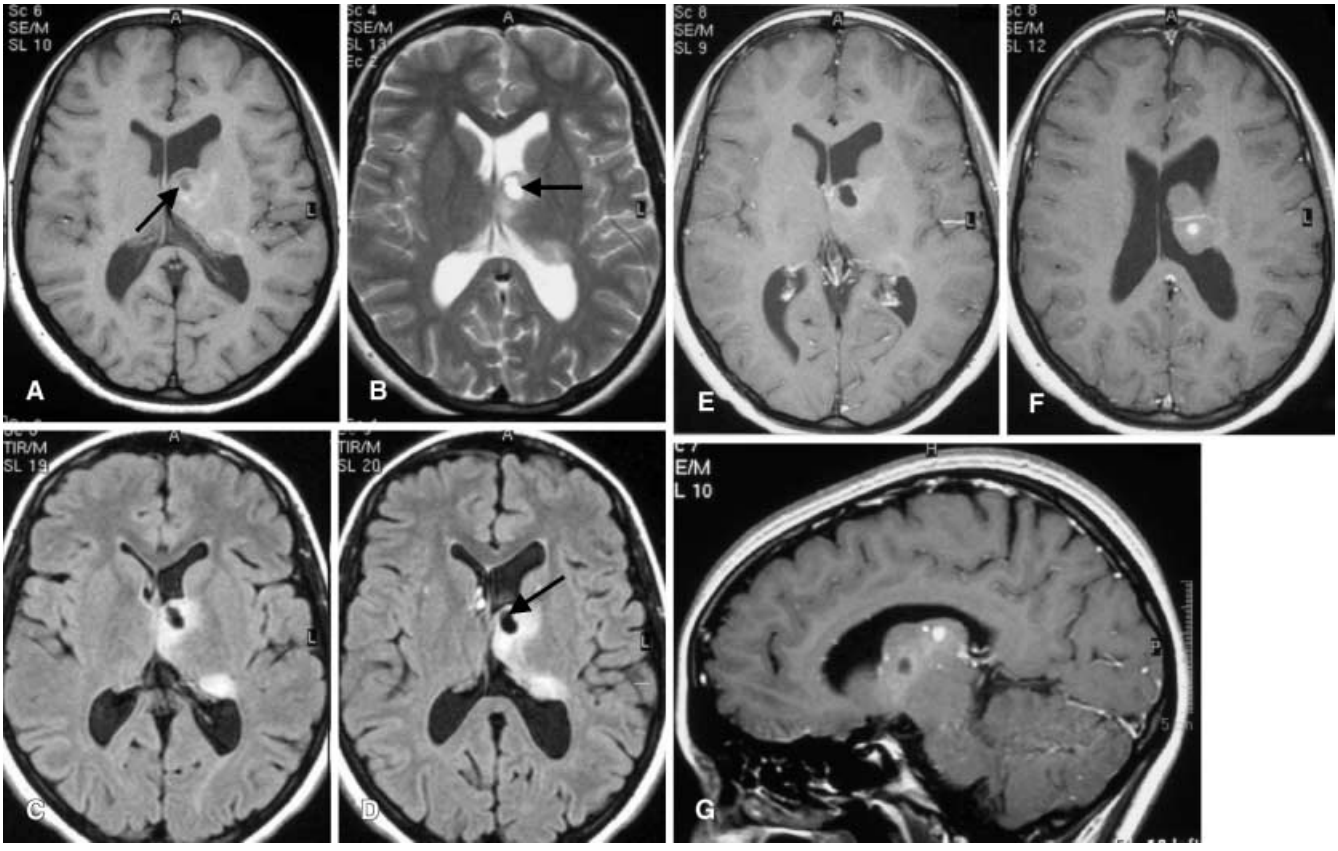

Fig. 12A–G Seventeen-year-old female; ganglioglioma of left thalamus (pilocytic variant). **A** Axial SE T1-WI. **B** Axial SE T2-WI. **C**, **D** Axial T-FLAIR. **E**, **F** Axial SE T1-WI after contrast injection. **G** Sagittal SE T1-WI after contrast injection. The ventral and dorso-lateral nuclei of the left thalamus are involved due to an inhomogeneous tumor that abuts on the lateral ventricle. The lesion appears hyperintense on FLAIR images, with little foci of enhancement after gadolinium injection. A small cystic component is evident in the anterior portion of the tumor (*arrow* in **A**, **B** and **D**)

extensive vasogenic edema. CT density and MR signal intensity of the thalamic GBM are markedly inhomogeneous, usually with central necrosis, possible cavitation and fluid/fluid level, and frequent hemorrhage at any stage of the evolution (Fig. 10). MRI is distinctly superior to CT in defining the composition of the heterogeneous GBM, especially on T2-WI and post-contrast images: the recognition of necrosis is more distinct, showing heterogeneous intensity, degraded blood products, and poor contrast enhancement. At the same time the proliferating peripheral areas exhibit relatively low intensity on T2-WI (high cellularity) and strong contrast enhancement. Despite its circumscribed appearance, thalamic GBM may have small finger-like marginal extensions that represent their tendency to infiltrate adjacent tissues or evolve, producing intraventricular and craniospinal leptomeningeal CSF seeding.

Oligondendrogliomas and mixed gliomas

Oligondendrogliomas (ODG) are rare in children ranging from 1 to 3% of all pediatric CNS tumors [11]; thus we prefer to present ODG together with mixed astrocytic/oligodendroglial tumors (MG) which show very similar imaging patterns. The pathological features of ODG and MG provide the basis for imaging findings: they are circumscribed, heterogeneous lesions that frequently contain calcification, cysts, and hemorrhage or blood degradation products (Fig. 11); calcification is the most typical finding of ODG, despite some reports that found calcification to be less common in children than in adults. Thus, a thalamic ODG or MG resembles a malignant astrocytoma, but appears more circumscribed and more frequently calcified, and without necrosis. The signal intensity is heterogeneous on both T2- and T1-WI, because calcification and proteinaceous cystic content can also induce hyperintensity counterparts in T1-WI; obviously the distinct recognition of calcification is based upon CT. Due to the heterogeneity of CT density and MR signal intensity, it is not possible to differentiate between the more common low-grade (grade II) ODG and MG and the more malignant grade III ones: the extent of edema and rapid increase in size support the hypothesis of the tumor being anaplastic.

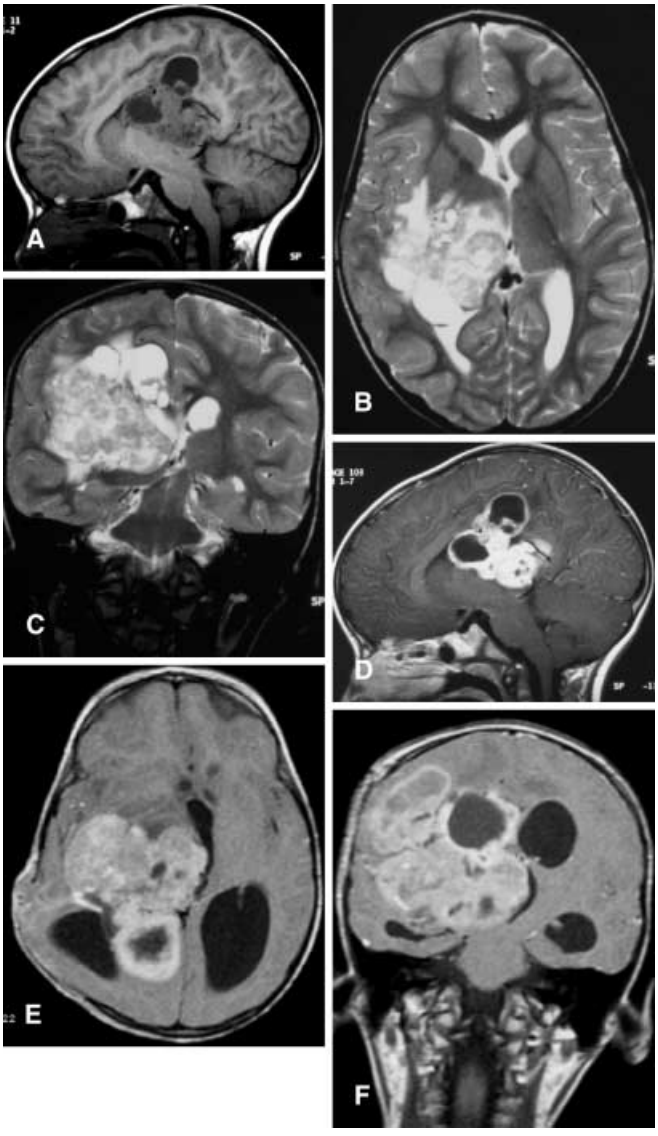

Fig. 13A–F Two-year-old female; atypical teratoid-rhabdoid tumor. **A** Sagittal SE T1-WI. **B** Axial SE T2-WI. **C** Coronal FSE T2-WI. **D–F** Post-operative (minimal resection) sagittal, axial, and coronal SE T1-WI after contrast injection. A huge inhomogeneous deep located mass has its epicenter in the right thalamus. The lesion shows multiple macro- and micro-cystic components, as well necrosis. The signal of the solid component appears mildly hypointense on T1-WI, and mildly hyperintense on T2-WI (suggesting high cellularity), with intense contrast enhancement

Gangliogliomas and neuronal/mixed neuronal tumors

Gangliogliomas (GG) and similar neuronal/mixed neuronal tumors represent approximately 1–2% of all CNS tumors [5], but are almost exclusively confined to children and very young adults. The thalamic location is exceedingly rare and a definite preoperative neuroradiological diagnosis is virtually impossible because their imaging features are similar to their astrocytic counterparts (pilocytic, fibrillary, anaplastic), and because in the deep location they lack the calvarial scalloping that supports correct recognition in the typically superficial temporal location. They are usually well circumscribed benign and non-progressive tumors; in the rarely encountered thalamic GG, the cystic appearance predominates, with sharp margins and focal areas of contrast enhancement, probably corresponding to pilocytic components; again calcification results in areas of T1-hyperintensity and signal intensity is extremely variable on T2-WI (Fig. 12). Because of their deep location and benign clinical behavior, long-term imaging follow-up is often carried out, and no progression has been confirmed.

Atypical teratoid-rhabdoid tumors

This recently described highly malignant tumor almost exclusively affects infants and children younger than 3 years of age. It is included within the group of embryonal tumors, together with the more common medulloblastomas and primitive neuroectodermal tumors. The microscopic distinctive feature of atypical teratoid-rhabdoid tumors (ATR) is the presence of rhabdoid cells, while on immunochemistry it exhibits positivity to vimentin, smooth muscle actin, and cheratin. ATR has been described as being found in both supratentorial and infratentorial locations; supratentorial ATRs usually occur in the deep white matter, but thalamic location/involvement is possible. At diagnosis, these malignant tumors appear as a large heterogeneous mass (Fig. 13) that contains necrosis, areas of high cellularity (hypointense on T2-WI), and hemorrhage; after contrast injection intense, non-homogeneous contrast enhancement is usually observed. Edema and mass effect are extensive. The prognosis of children with ATR is poor and CSF seeding is common.

Multifocal/multicentric gliomas with thalamic involvement

Besides the bilateral thalamic gliomas mentioned above, the thalami are frequently involved in multifocal/multicentric gliomas, and in the gliomatosis cerebri (GC) [10]. After the WHO acceptance of the definition of gliomatosis cerebri [10] the widespread and superior sensitivity of MRI allowed an increased number of GC diagnoses. In our two biopsy or autopsy-proven pediatric cases of GC (Fig. 14), the thalamus was always involved. In both cases the thalamus involved appeared diffusely enlarged with moderate hyperintensity on T2-WI and without contrast enhancement; in both cases, the disease appeared to be progressing rapidly, with the evolution of the largest subcortical locations toward anaplasia and death, despite aggressive chemo-radiation. The

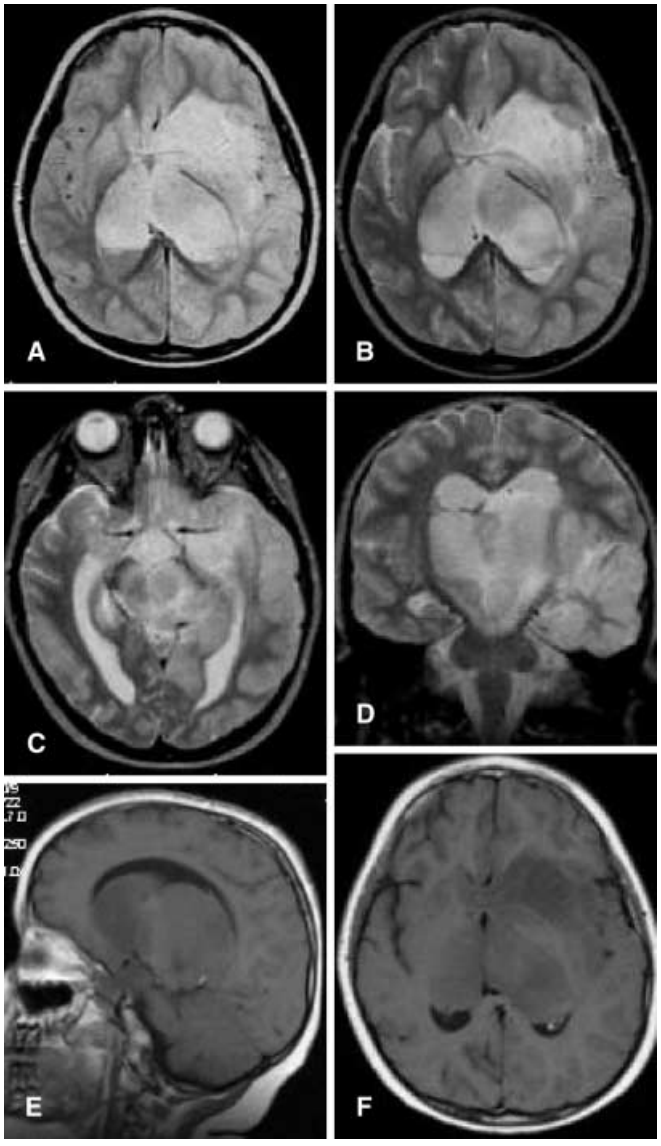

Fig. 14A–F Four-year-old male; diffuse bilateral anaplastic astrocytoma (namely gliomatosis cerebri). **A–C** Axial SE PD and T2-WI. **D** Coronal FSE T2-WI. **E**, **F** Sagittal and axial SE T1-WI after contrast injection. The diffusely infiltrating disease involves predominantly the basal ganglia (both thalami, the left lentiform nucleus and the head of left caudate nucleus), which are swollen, with hypointense signal on T1-WI, hyperintensity on the long TR images, without enhancement after contrast-injection. Moreover the infiltration extends into the hypothalamus, the anterior commissure and the left insula

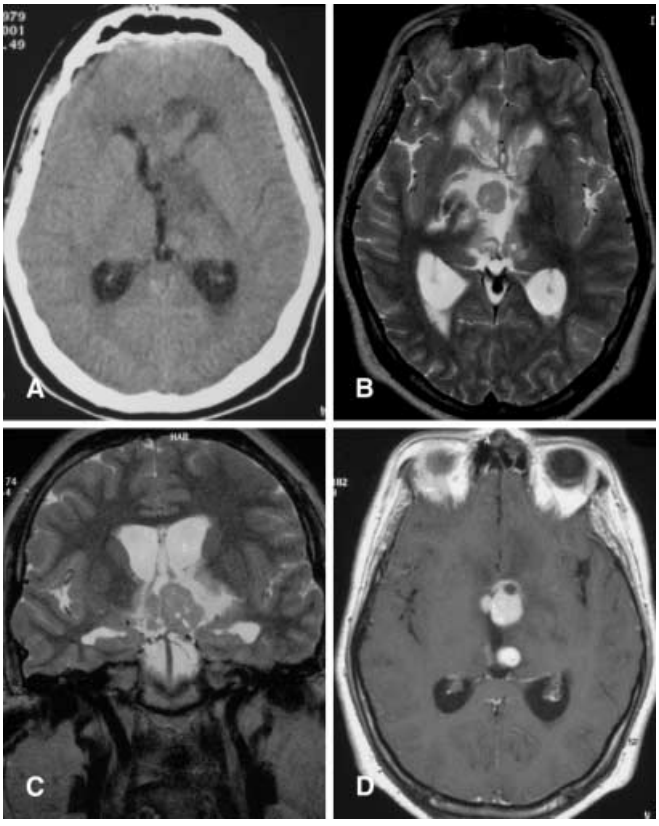

Fig. 15A–D Seventeen-year-old male; diffuse germ cell tumor (germinoma) with bilateral thalamic involvement. **A** Axial CT scan. **B**, **C** Axial and coronal SE T2-WI. **D** Axial SE T1-WI after contrast injection. Multiple nodules are present along the wall of the third ventricle, involving the region of Monro's foramina and resulting in obstructive biventricular hydrocephalus; tumor tissue is characterized by iso-hyperdensity on CT, inhomogeneous iso-hypointensity on T2-WI (rich cellularity), and marked enhancement after contrast injection. Both thalami are infiltrated

thalami may also be involved in more benign multifocal glial tumors in which the focal lesions show low-grade astrocytic, non-malignant ODG or neurocytoma. Thalamic lesions in such cases have extremely variable imaging features, with possible calcification and focal contrast enhancement, usually with absent or moderate edema and mass effect. Obviously in such multifocal/multicentric lesions, MRI is of the utmost importance for clinical surveillance and for assessing the effects of treatment.

Germ cell tumors

Fifteen percent of germ cell tumors (GCT) occur in the basal ganglia, especially in the thalami; as in the case of the most common pineal location, there is a clear predominance in males [16, 21]. Most thalamic GCTs actually originate outside the thalami and infiltrate the thalami from the posterior or anterior walls of the third ventricle. Wherever the epicenter of the growth is located, GCTs show a typical infiltrative pattern and CT density/MRI signal intensity enable the differential diagnosis with neuroepithelial thalamic tumors. In fact, the rich cellularity of GCTs (predominantly small lymphocytic-like cells and large polygonal cells) is represented by

moderate hyperdensity on unenhanced CT, relative hypointensity on T2-WI, and almost homogeneous contrast enhancement (Fig. 15). The infiltrating tumor appears almost homogeneous, with small cystic areas in large lesions and moderate perilesional edema. When GCT is suspected, contrast-enhanced MRI must routinely include the spine, due to the frequency of multiple locations and leptomeningeal CSF seeding. The main differential diagnosis is with primitive CNS lymphoma.

Lymphoma

Historically, brain lymphomas (LY) were uncommon, especially in infants and children. As well as the effect due to the diffusion of the acquired immunodeficiency syndrome (AIDS), a general increase in the frequency of primary CNS lymphomas has been observed in the last 20 years, which has also affected children [21]. A significant percentage of CNS lymphomas are located in the deep brain regions and the thalami. The neuroradiological diagnosis is facilitated by the knowledge of a preexisting immunodeficiency condition, but in most cases thalamic lymphomas show neuroimaging features that allow differentiation from the more common glial thalamic tumors. As in GCT, the high cellularity and infiltrating behavior are significant distinctive features shown by hyperdensity on CT (without intravenous contrast) and relative hypointensity on T2-WI [15, 21]; edema is usually conspicuous and central necrosis as well as hemorrhage may be found due to perivascular growth and infiltration. Brain lymphomas may be multicentric [21] and disseminate through the CSF. The differential diagnosis with GCT may be difficult, although the latter is more commonly located on the midline.

Basic neuroimaging patterns of thalamic tumors (a guide to the differential diagnosis)

To summarize the neuroradiologic findings described above, we attempted to define basic neuroimaging patterns of thalamic tumors that rapidly address the differential diagnosis (by reducing the possible hypotheses). Obviously this simplified approach should be considered a "quick guide", and the resulting diagnosis should be supported by matching the neuroradiological findings to the clinical and epidemiological data.

Pattern I

A solid tumor, hypodense on unenhanced CT, hypo-isointense on T1-WI, and hyperintense on T2-WI, with moderate/absent edema, and without contrast enhancement. These features strongly suggest diffuse non-anaplastic astrocytoma. However, when there is extensive infiltration involving adjacent structures or both thalami, despite the lack of contrast enhancement, the most reliable diagnosis is anaplastic astrocytoma. Gliomatosis cerebri may be suggested when the tumor involves other cortical/subcortical areas besides the thalamus when they enlarge.

Pattern II

A solid tumor, with or without cystic counterparts, that appears hypodense on unenhanced CT, hypointense on T1-WI, hyperintense on T2-WI, and with contrast enhancement. This pattern is encountered in very different tumors with dramatically different prognoses, but correct diagnosis can be provided by considering the following "sub-patterns":

1. If the margins of the tumor are well defined and areas of contrast enhancement appear homogeneous, the most reliable diagnosis is pilocytic astrocytoma or ganglioglioma (less common)
2. If the margins are ill defined, with infiltrative behavior, and contrast enhancement is patchy and/or non-homogeneous, anaplastic astrocytoma is the most reliable diagnosis
3. If the features described above are associated with necrosis, hemorrhage, and extensive edema, glioblastoma multiformis is the most likely diagnosis; as an alternative, ATR may be proposed in infants

Pattern III

A solid tumor, with or without cystic components, with calcifications on CT, non-homogeneous hypointensity on T1-WI and hyperintensity on T2-WI, and with contrast enhancement. Oligodendroglioma or mixed oligo-astrocytoma are possible diagnoses, but astrocytoma or anaplastic astrocytoma cannot be excluded.

Pattern IV

A solid or predominantly solid tumor, hyperdense on unenhanced CT, hypo/isointense on T1-WI, isointense or hypointense on T2-WI, with contrast enhancement, infiltrating the walls of the posterior third ventricle. This pattern is strongly suggestive of a diagnosis of germ cell tumor, even if the pineal area is not involved; however, lymphoma should be considered as the second option.

References

1. Allen JC (2000) Initial management of children with hypothalamic and thalamic tumors and the modifying role of neurofibromatosis-l. Pediatr Neurosurg 32:154–162
2. Aronen H, Gazit I, Buchbinder B, et al (1995) Cerebral blood volume maps of gliomas: comparison with tumor grade and histologic findings. Radiology 191:41–51
3. Arseni C (1958) Tumors of the basal ganglia. Their surgical treatment. Arch Neurol Psychiatry 80:18–24
4. Bernstein M, Hoffmann HJ, Halliday WC, Hendrick EB, Humphreys RP (1984) Thalamic tumors in children. Long-term follow-up and treatment guidelines. J Neurosurg 61:649–656
5. Castillo M (1998) Gangliogliomas: ubiquitous or not? Am J Neuroradiol 19:807–809
6. Cheek WR, Taveras M (1966) Thalamic tumors. J Neurosurg 24:505–513
7. Drake JM, Joy M, Goldenberg A, Kreindler D (1991) Computer- and robot-assisted resection of thalamic astrocytomas in children. Neurosurgery 29:27–33
8. Duffner PK, Knischer JP, Horowitz ME (1998) Second malignancies in young children with primary brain tumors following treatment with prolonged postoperative chemotherapy and delayed irradiation: a pediatric oncology study group. Ann Neurol 44:313
9. Esteve F, Grand S, Rubin C, Hoffmann D, Pasquier B, Graveron-Demilly D, Mahdjoub R, Le Bas JF (1999) MR spectroscopy of bilateral thalamic gliomas. Am J Neuroradiol 20:876–881
10. Felsberg GJ, Silver SA, Brow MT, Tien RD (1994) Gliomatosis cerebri; radiologic-pathologic correlation. Am J Neuroradiol 15:1745–1753
11. Lee YY, Van Tassel P (1989) Intracranial oligodendrogliomas: imaging findings in 35 untreated cases. Am J Neuroradiol 10:119–127
12. Luyten PR, Marien Ad IH, Heindel W, et al (1990) Metabolic imaging or patients with intracranial tumors: 1H-MR spectroscopic imaging and PET. Radiology 176:791–799
13. Lyons MK, Kelly PJ (1992) Computer-assisted stereotactic biopsy and volumetric resection of thalamic pilocytic astrocytomas. Report of 23 cases. Stereotact Funct Neurosurg 59:100–104
14. Matsumoto K, Higashi H, Tomita S, Furuta T, Ohmoto T (1995) Resection of deep-seated gliomas using neuroimaging for stereotactic placement of guidance catheters. Neurol Med Chir Tokyo 35:148–155
15. Moschini M, Tartaglione T, Rollo M, et al (1994) Diagnostic imaging of HIV-related intracranial expansive lesions. Rays 19:51–67
16. Ono N, Inoue HK, Naganuma H, et al (1996) Diagnosis of germinal neoplasm in the thalamus and basal ganglia. Surg Neuro1 26:24–28
17. Ostegaard L, Hochberg FH, Rabinov JD, et al (1999) Early changes measured by MRI in cerebral blood flow, blood volume and blood-brain barrier following treatment in patients with brain tumors. J Neurosurg 90:300–305
18. Packer RJ, Ater J, Allen J, Phillips P, Geyer R, Nicholson HS, Jakacki R, Kurczynski E, Needle M, Finlay J, Reaman G, Boyett JM (1997) Carboplatin and vincristine chemotherapy for children with newly diagnosed progressive low-grade gliomas. J Neurosurg 86:747–754
19. Scerrati M, Roselli R, Iacoangeli M, Pompucci A, Rossi GF (1996) Prognostic factors in low grade (WHO grade II) gliomas of the cerebral hemispheres: the role of surgery. J Neurol Neurosurg Psychiatry 61:291–296
20. Siffert J, Allen JC (2000) Late effects of therapy of thalamic and hypothalamic tumors in childhood: vascular, neurobehavioral and neoplastic. Pediatr Neurosurg 33:105–111
21. Simonetti L, De Simone MR, Cerase A, Cirillo S, Colosimo C (1996) Neoplasms of the basal ganglia. Rays 21:70–86
22. Steiger HJ, Gotz C, Schmid-Elsaesser R, Stummer W (2000) Thalamic astrocytomas: surgical anatomy and results of a pilot series using maximum microsurgical removal. Acta Neurochir (Wien) 142:1327–1336; discussion 1336–1337
23. Wald SL, Fogelson H, McLaurin RL (1982) Cystic thalamic gliomas. Childs Brain 9:381–393
24. Yanaka K, Kamezaki T, Kobayashi E, Matsueda K, Yoshii Y, Nose T (1992) MR imaging of diffuse glioma. Am J Neuroradiol 13:349–351
25. Yoshida M, Fushiki S, Takeuchi Y, Takanashi M, Imamura T, Shikata T, Morimoto A, Konishi K, Miyazaki A, Sawada T (1998) Diffuse bilateral thalamic astrocytomas as examined serially by MRI. Childs Nerv Syst 14:384–388